

Provided for non-commercial research and education use.  
Not for reproduction, distribution or commercial use.



This article appeared in a journal published by Elsevier. The attached copy is furnished to the author for internal non-commercial research and education use, including for instruction at the authors institution and sharing with colleagues.

Other uses, including reproduction and distribution, or selling or licensing copies, or posting to personal, institutional or third party websites are prohibited.

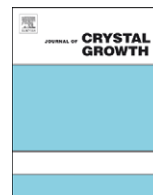
In most cases authors are permitted to post their version of the article (e.g. in Word or Tex form) to their personal website or institutional repository. Authors requiring further information regarding Elsevier's archiving and manuscript policies are encouraged to visit:

<http://www.elsevier.com/copyright>



Contents lists available at ScienceDirect

## Journal of Crystal Growth

journal homepage: [www.elsevier.com/locate/jcrysgro](http://www.elsevier.com/locate/jcrysgro)Fabrication and microstructure of Cu<sub>2</sub>O nanocubesY.Q. Wang<sup>a,b,c,\*</sup>, W.S. Liang<sup>c</sup>, A. Satti<sup>a</sup>, K. Nikitin<sup>a</sup><sup>a</sup> School of Chemistry and Chemical Biology, University College Dublin, Belfield, Dublin 4, Ireland<sup>b</sup> Department of Materials, Imperial College London, Prince Consort Road, London, SW7 2AZ, United Kingdom<sup>c</sup> The Cultivation Base for the State Key Laboratory, Qingdao University, No. 308 Ningxia Road, Qingdao 266071, PR China

## ARTICLE INFO

## Article history:

Received 28 September 2009

Received in revised form

13 December 2009

Accepted 12 January 2010

Communicated by K. Nakajima

Available online 20 January 2010

## Keywords:

A1. Characterization

A1. Surface structure

B1. Nanomaterials

B2. Semiconducting materials

## ABSTRACT

Cu<sub>2</sub>O nanocubes (edge length of 6 to 250 nm) have been produced by annealing a copper grid at 300 °C in air with the presence of tetraoctylammonium bromide (TOAB)-stabilized gold nanoparticles. The microstructure of the nanocubes has been investigated in details using conventional and high-resolution transmission electron microscopy (HRTEM), and chemical analysis has been performed using energy dispersive X-ray spectroscopy (EDS) and electron energy-loss spectroscopy (EELS) in the scanning transmission electron microscopy (STEM). Based on the experimental results, a possible growth mechanism is proposed.

© 2010 Elsevier B.V. All rights reserved.

## 1. Introduction

Nanoparticles have attracted considerable attention due to their novel physical and chemical properties, and their potential applications in next generation devices. Fabrication of particles with well-defined and controlled shapes and sizes will be crucial to such applications. To date considerable effort has been directed towards synthesis of nanomaterials with different shapes, such as nanoparticles [1], nanowires [2], nanobelts [3] and nanocubes [4,5].

Recently cuprous oxide, Cu<sub>2</sub>O, nanostructures have attracted significant attention as a p-type semiconductor with a direct band-gap of ~2.0 eV for potential applications in solar energy conversion and catalysis [6,7]. Different shapes of Cu<sub>2</sub>O nanoparticles have been synthesized by various methods [8–10]. However, no detailed investigation on the microstructure and growth mechanism of the Cu<sub>2</sub>O nanocubes has been reported.

In this paper, we report the fabrication and microstructural characterization of Cu<sub>2</sub>O nanocubes. These nanocubes were produced by annealing in air at 300 °C for 40 min a carbon-film-coated copper grid on which tetraoctylammonium bromide (TOAB)-stabilized gold nanoparticles were dispersed. Two major morphologies have been observed for the nanocubes: one being nearly a perfect cube, and the other being a truncated structure. Faceting has been commonly observed in the projected images

(viewed along the <100> or <110> direction) of the nanocubes. An excess of TOAB and an oxygen environment are crucial factors for the formation of these nanocubes. A possible formation mechanism is also discussed.

## 2. Experimental

## 2.1. Synthesis and characterization of gold nanoparticles

The gold nanoparticles were synthesized via a modification of a literature protocol [11,12]. Briefly, an aqueous solution of HAuCl<sub>4</sub>·3H<sub>2</sub>O (0.03 M, 6 mL) was added to a solution of TOAB in toluene (0.15 M, 6 mL). The yellow aqueous phase became colorless, and the toluene phase turned orange as a result of phase transfer and complexing of [AuCl<sub>4</sub>]<sup>-</sup> with tetraoctylammonium cations. After stirring for 10 min at room temperature, a freshly prepared aqueous solution of sodium borohydride, NaBH<sub>4</sub> (0.26 M, 6 mL), was added dropwise into the reaction mixture over a period of 30 min, after which the mixture was vigorously stirred for additional 30 min. Subsequently, the organic phase was separated and was washed with 1% H<sub>2</sub>SO<sub>4</sub> once and then with distilled-deionised water five times. Finally the organic phase was dried using MgSO<sub>4</sub> and filtered through a filter paper. The as-synthesized gold nanoparticles were characterized using conventional transmission electron microscopy (TEM). The specimen for TEM observation was prepared by evaporating a drop (5 μL) of the nanoparticle dispersion onto a carbon-film-coated copper grid.

\* Corresponding author at: The Cultivation Base for the State Key Laboratory, Qingdao University, No. 308 Ningxia Road, Qingdao 266071, PR China.  
Tel.: +86 532 83780318

E-mail address: [yqwang@qdu.edu.cn](mailto:yqwang@qdu.edu.cn) (Y.Q. Wang).

## 2.2. Fabrication and TEM characterization of $\text{Cu}_2\text{O}$ nanocubes

To prepare the  $\text{Cu}_2\text{O}$  nanoparticles, the copper grid covered with the TOAB-stabilized gold nanoparticles was placed in an oven and the temperature was raised to 300 °C at a heating rate of 1 °C/s. The temperature was kept constant at 300 °C for 40 min. The final product appeared shiny on the copper grid and was examined extensively using conventional and high-resolution TEM. The bright field (BF) imaging and *in-situ* heating experiment were performed on a JEOL JEM-2000EX electron microscope. The selected-area electron diffraction (SAED), high-resolution TEM (HRTEM), high-angle annular dark field (HAADF), energy

dispersive X-ray spectroscopy (EDS) and electron energy-loss spectroscopy (EELS) were carried out using an FEI Titan 80-300 scanning transmission electron microscope (STEM).

## 3. Results and discussion

Fig. 1 shows typical BF images and corresponding SAED patterns of gold nanoparticles before heating and the nanocubes formed after heating. It can be seen from Fig. 1(a) that most of the gold nanoparticles are spherical with an average diameter of about 5.2 nm. The corresponding SAED pattern (Fig. 1(b))

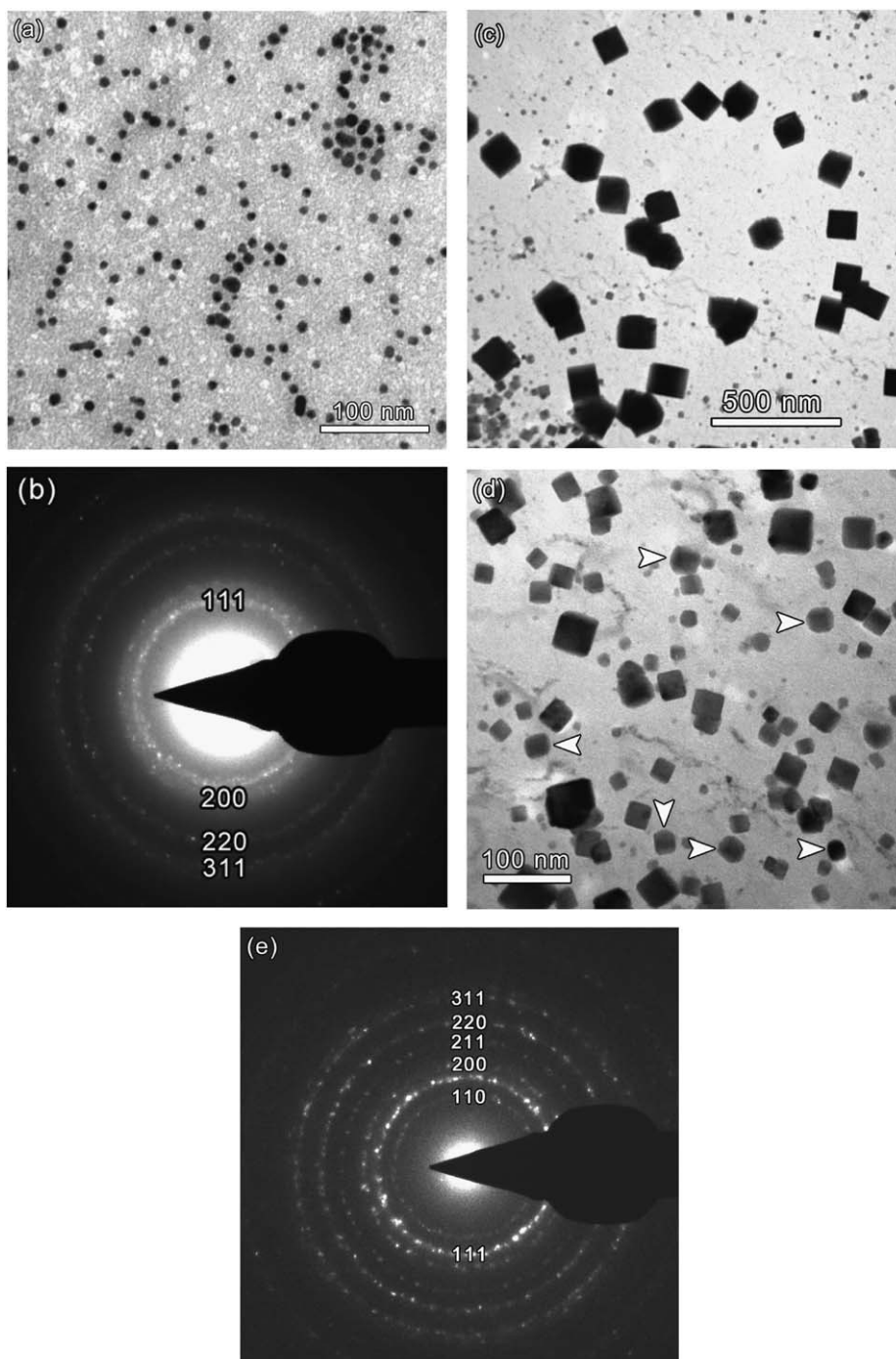


**Fig. 1.** Typical BF image (a) and corresponding SAED pattern (b) of gold nanoparticles; typical BF images (c) and (d) and corresponding SAED pattern (e) taken from nanocubes.

confirms that before heating, the nanoparticles are of pure gold. Fig. 1(c) shows that after heating, nearly all the nanoparticles have transformed into cubic morphologies. The edge length of the nanocubes ranges from 6 to 250 nm. Careful examination of Fig. 1(d) shows that some nanocubes (indicated by white arrows) have truncated corners. It should be noted that after heating, the carbon film is intact and most of the nanocubes are located close to the edge of the grid bar rather than in the center of the square. The SAED pattern acquired from the nanocubes (Fig. 1(e)) indicates that they have a different structure from pure gold (Fig. 1(b)).

To clarify the composition and structure of these nanocubes, chemical analyses were performed in STEM mode on a Titan 80-300 STEM operating at 300 kV. Fig. 2(a) shows an HAADF image of the nanocubes. EDS spectra show that the as-synthesized nanoparticles are of pure gold, while the nanocube is mainly composed of Cu and O with a negligible amount of gold (Fig. 2(b)). Quantification of the EDS spectrum from a single nanocube shows that the ratio of Cu and O is  $2.00 \pm 0.06:1$ , suggesting that the nanocubes have a chemical formula of  $\text{Cu}_2\text{O}$ . Fig. 2(c) shows a background-subtracted EELS spectrum acquired from a single nanocube, where two peaks at 532 and 931 eV correspond to O-K edge and Cu-L<sub>2,3</sub> edge, respectively. The data were recorded using convergence and collection angles of 9.5 and 9.75 mrad, respectively. With the X-ray diffraction data (JCPDS 5-667), the electron diffraction pattern in Fig. 1(d) can be indexed using the

lattice parameter of  $\text{Cu}_2\text{O}$  ( $a=4.269 \text{ \AA}$ ), consistent with the results of the chemical analyses.

To investigate the microstructure of the nanocubes, extensive HRTEM examinations were carried out on a Titan 80-300 STEM. All the nanocubes are single crystals, and no planar defects such as twins and stacking faults are observed inside them. Several  $\langle 001 \rangle$  or  $\langle 110 \rangle$  zone-axis HRTEM images of the cubes are shown in Fig. 3. As noted earlier, some nanoparticles have a nearly perfect cubic structure, while the others have a truncated structure.

Fig. 3(a and b) shows two examples of a nearly perfect cube, one being viewed from the  $[001]$  direction and the other being viewed from the  $[110]$  direction. The nanoparticle in Fig. 3(a), viewed from the  $[001]$  direction, has a projected shape of a nearly perfect square, indicating that this particle has a nearly perfect cubic structure in three dimensions. It has an edge length of around 33 nm, and straight edges with  $\{100\}$  and  $\{010\}$  facets. However, near the corners, it shows a curved rather than a right-angled configuration, and the facets around the corners are  $\{110\}$  planes. If viewed from the  $[110]$  direction, the nanocubes should have a projected shape of a rectangle with the edge length ratio of  $\sqrt{2}$ . One example is shown in Fig. 3(b). The edges are flat with  $\{110\}$  and  $\{001\}$  facets, and the length ratio of the edges is very close to 1.41, indicating that this particle is also a nearly perfect cube in three dimensions. The interplanar spacings of the  $\{111\}$ ,  $\{001\}$  and  $\{110\}$  planes measured from the HRTEM

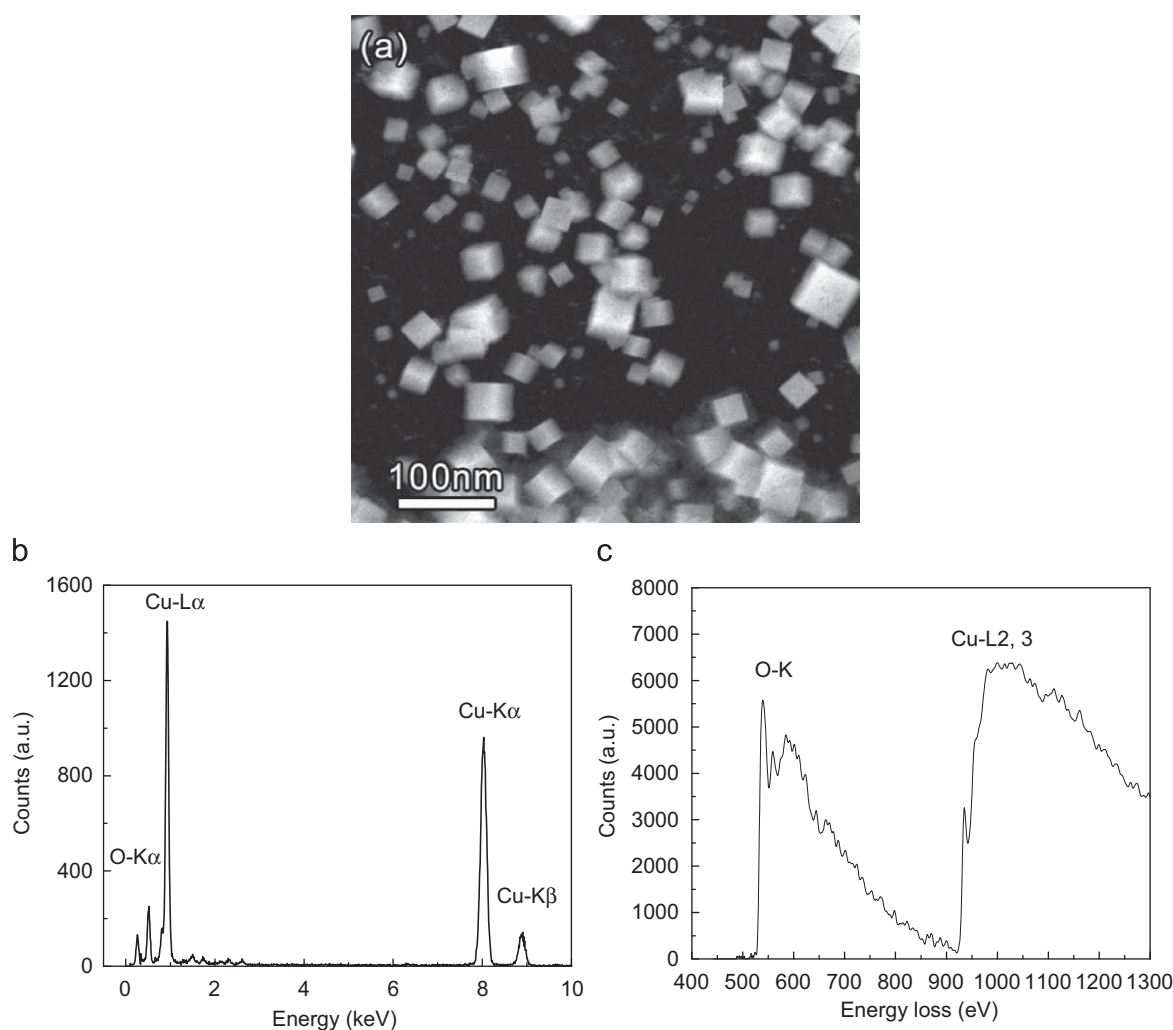
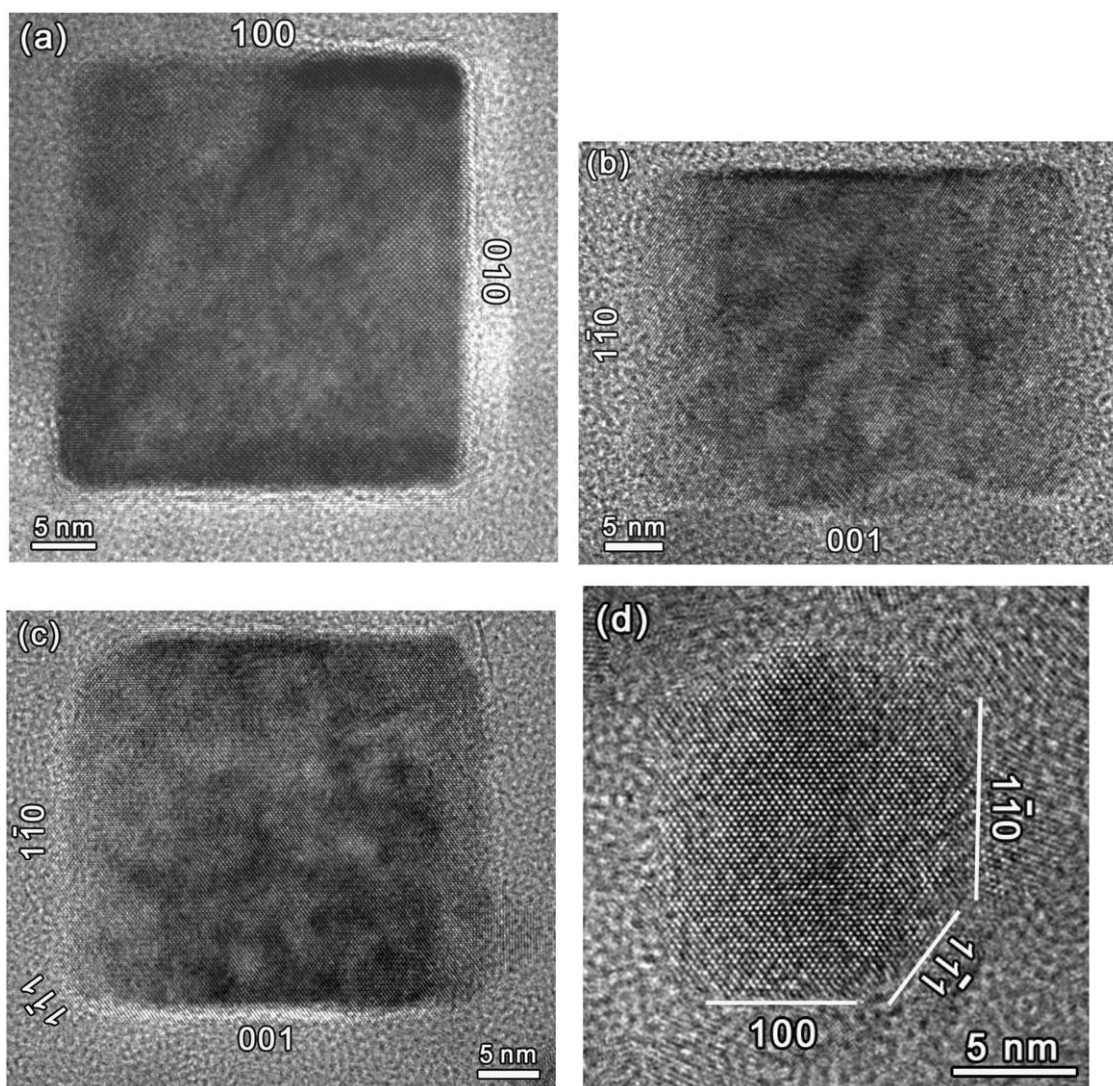


Fig. 2. (a) A typical HAADF image of the nanocubes; (b) EDS spectrum from a single nanocube; (c) EELS spectrum from a single nanocube.



**Fig. 3.** (a) [0 0 1] and (b) [1 1 0] zone-axis HRTEM images of nearly perfect  $\text{Cu}_2\text{O}$  nanocubes; (c) and (d) [1 1 0] zone-axis HRTEM images of truncated  $\text{Cu}_2\text{O}$  nanocubes.

images are 2.46, 4.27 and 3.02 Å, respectively, consistent with the theoretical values for  $\text{Cu}_2\text{O}$ . It is very interesting to find that nearly all nanoparticles adopt a cubic morphology. This can be explained from the energy optimization of the surfaces for the particles. In the simple cubic  $\text{Cu}_2\text{O}$  crystal, {1 0 0} planes are low-energy surfaces. Therefore, it is understandable that the  $\text{Cu}_2\text{O}$  nanoparticles form a cubic rather than a spherical morphology.

For some  $\text{Cu}_2\text{O}$  nanoparticles, they have a cubo-octahedral structure, which is a truncated cubic structure. Two examples are shown in Fig. 3(c and d). Viewed from the [1 1 0] direction, they also have a projected shape of a rectangle, similar to that in Fig. 3(b). However, the edges are not very straight and the edge length ratio is less than 1.41, which is different from that in Fig. 3(b). In Fig. 3(c), the nanoparticle, viewed from the [1 1 0] direction, has a projected shape of a rectangle with four curved corners. This indicates that the particle in Fig. 3(c) is not a cube in three dimensions, but a truncated cubic structure. The facets can be indexed as {1 1 0} and {0 0 1}, and the four corners with the curved morphologies can be indexed as {1 1 1} facets. In Fig. 3(d), the nanoparticle shows a more heavily truncated structure. From Fig. 3(d), the {1 0 0}, {1 1 0} and {1 1 1} facets can be seen, although not so evident as those in Fig. 3(c). The particle starts to show up a rectangular morphology.

It has been found that the concentration of TOAB to synthesize the gold nanoparticles and the concentration of the gold nanoparticles on the copper grid are critical to the formation of  $\text{Cu}_2\text{O}$  nanocubes. During this experiment, the TOAB is taken in excess and the concentration of the gold nanoparticles on the copper grid is very low. This might be the reason why no gold nanoparticles show up in the HRTEM images after heating. The investigation of the influence of the synthesis conditions (especially TOAB concentration) and the concentration of gold nanoparticles on the microstructure of  $\text{Cu}_2\text{O}$  nanocubes is in progress and the results will be reported elsewhere.

It is apparent that the presence of oxygen in the environment is crucial for the formation of the cubes, since it might provide the source of oxygen to oxidize the copper grid into cuprous oxide. To prove this point, we performed the *in-situ* heating of the same batch of gold nanoparticles on a JEOL JEM-2000EX electron microscope. Considering the limited heat transfer from the sample holder to the copper grid, we carried out the experiment at around 500 °C. The *in-situ* TEM observations show that the gold nanoparticles are not transformed into gold nanocubes; however, the smaller gold particles can coalesce together and form bigger ones. This indicates that the gold nanoparticles will not transform into gold nanocubes in vacuum (around  $10^{-7}$  Torr), which further

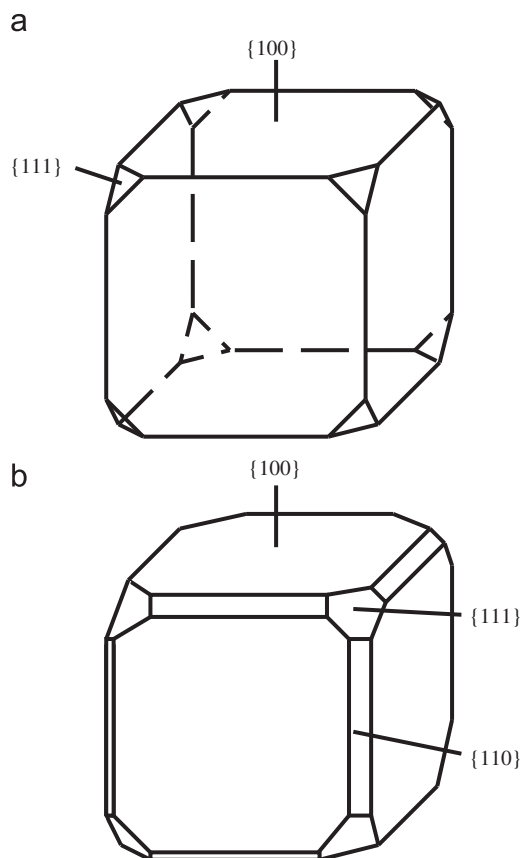


**Fig. 4.** The 3-dimensional geometrical shapes of (a) nearly perfect  $\text{Cu}_2\text{O}$  nanocubes; (b) truncated  $\text{Cu}_2\text{O}$  nanocubes.

strengthens the above finding that an environment with oxygen is essential for the formation of the  $\text{Cu}_2\text{O}$  nanocubes. In addition, a high temperature ( $300\text{ }^\circ\text{C}$ ) is also very important for the formation of the cubes. From our TEM observation, the nanoparticles are still pure gold after the heat treatment at  $200\text{ }^\circ\text{C}$  for 40 min, which is consistent with the report on the influence of heat treatment on the size evolution of gold nanoparticles [13]. Moreover, if there is no gold nanoparticle on the copper grid, no nanocube will be observed. This indicates that the copper grid can only be oxidized into  $\text{Cu}_2\text{O}$  nanocubes at a relatively high temperature ( $300\text{ }^\circ\text{C}$ ) in the presence of gold nanoparticles and oxygen. In addition, no  $\text{CuO}$  nanostructures were observed. The temperature of  $300\text{ }^\circ\text{C}$  is not high enough for the formation of a dominant  $\text{CuO}$  phase, which is consistent with our TEM observations and the results reported in the literature [14].

Based on the experimental results, we proposed a possible growth mechanism for the  $\text{Cu}_2\text{O}$  nanocubes as follows. Firstly, the growth of  $\text{Cu}_2\text{O}$  occurs on the surface of the Cu grid. When the temperature is approaching  $300\text{ }^\circ\text{C}$ , the oxygen in atmosphere can oxidize the copper grid into  $\text{Cu}_2\text{O}$  ( $4\text{Cu} + \text{O}_2 \rightarrow 2\text{Cu}_2\text{O}$ ). Then  $\text{Cu}_2\text{O}$  particles grow bigger and transform into the shape of nanocubes due to surface energy optimization. Finally, the nanocubes exfoliate from the growth layer of the Cu grid surface onto the amorphous carbon film. This can explain why all the nanocubes are located close to the edge of the Cu grids.

Another interesting finding is that some cubes have a nearly perfect cubic structure while the others have a truncated structure. Fig. 4(a) depicts a nearly perfect cube (Fig. 3(a and b))

while Fig. 4(b) displays a truncated structure (Fig. 3(c and d)). The schematic diagram also shows the relationship of particle shape with the ratio of the  $\{1\ 1\ 1\}$  facet area to the  $\{1\ 0\ 0\}$  facet area. The shape depends on the ratio of the growth rate in the  $\langle 1\ 0\ 0 \rangle$  direction to that in the  $\langle 1\ 1\ 1 \rangle$  direction. The particle shape is a perfect cube with right-angled corners with maximum area of the  $\{1\ 0\ 0\}$  facet and minimum area of the  $\{1\ 1\ 1\}$  facet. It has been shown in the cubo-octahedral nanoparticles [15,16] that the geometrical shapes are a function of the ratio of the growth rate in the  $\langle 1\ 0\ 0 \rangle$  direction to that in the  $\langle 1\ 1\ 1 \rangle$  direction. Another important feature of the nanocubes is that they are completely single crystalline. Usually planar defects such as twins and stacking faults are dominant in nanoparticles [17–19]; however, in these  $\text{Cu}_2\text{O}$  nanocubes, no twins or stacking faults have been observed, indicating that growth mechanism through coalescence of smaller nanoparticles into a bigger one is not valid in this system.

#### 4. Conclusions

In conclusion, well-faceted  $\text{Cu}_2\text{O}$  nanocubes with an edge length of 6 to 250 nm have been fabricated. The favourable facets are  $\{1\ 0\ 0\}$ ,  $\{1\ 1\ 0\}$  and  $\{1\ 1\ 1\}$  planes. The cubes have two major geometrical shapes in three dimensions: one being a nearly perfect cube, and the other being a truncated structure. The shape depends on the ratio of the growth rate in the  $\langle 1\ 0\ 0 \rangle$  direction to that in the  $\langle 1\ 1\ 1 \rangle$  direction.

#### Acknowledgements

This work was financially supported by European Union (UCD, Ireland), EPSRC (ICL, UK), the National Natural Science Foundation of China (Grant no. 10974105), the Scientific Research Award Foundation for Outstanding Young and Middle-Aged Scientists in Shandong Province (Grant no. BS2009CL005), and the Scientific Research Starting Foundation for the Introduced Talents at Qingdao University (Grant no. 06300701).

#### References

- [1] X. Peng, L. Manna, W. Yang, J. Wickham, E. Scher, A. Kadavanich, A.P. Alivisatos, *Nature* 404 (2000) 59.
- [2] A.M. Morales, C.M. Lieber, *Science* 279 (1998) 208.
- [3] Z.W. Pan, Z.R. Dai, Z.L. Wang, *Science* 291 (2001) 1947.
- [4] L.F. Gou, C.J. Murphy, *Nano Lett.* 3 (2003) 231.
- [5] Y. Sun, Y. Xia, *Science* 298 (2002) 2176.
- [6] J.A. Switzer, B.M. Maune, E.R. Raub, E.W. Bohannon, *J. Phys. Chem. B* 103 (1999) 395.
- [7] M. Hara, H. Hasei, M. Yashima, S. Ikeda, T. Takata, J.N. Kondo, K. Domen, *Appl. Catal. A* 190 (2000) 35.
- [8] P. Taneja, R. Chandra, R. Banerjee, P. Ayyub, *Scr. Mater.* 44 (2001) 1915.
- [9] E.G. Ponyatovskii, G.E. Abrosimova, A.S. Aronin, *Phys. Solid State* 44 (2002) 852.
- [10] W.Z. Wang, G.H. Wang, X.S. Wang, *Adv. Mater.* 14 (2002) 67.
- [11] M. Brust, M. Walker, D. Bethell, D.J. Schiffrin, R. Whyman, *J. Chem. Soc. Chem. Commun.* (1994) 801.
- [12] D.I. Gittins, F. Caruso, *Angew. Chem. Int. Ed.* 40 (2001) 3001.
- [13] T. Teranishi, S. Hasegawa, T. Shimizu, M. Miyake, *Adv. Mater.* 13 (2001) 1699.
- [14] C.H. Xu, C.H. Woo, S.Q. Shi, *Chem. Phys. Lett.* 399 (2004) 62.
- [15] Z.L. Wang, *J. Phys. Chem. B* 104 (2000) 1153.
- [16] T. Yan, Z.G. Shen, J.F. Chen, X.L. Liu, X. Tao, J. Yun, *Chem. Lett.* 8 (2005) 1196.
- [17] Y.Q. Wang, R. Smirani, G.G. Ross, *Nano Lett.* 4 (2004) 2041.
- [18] Y.Q. Wang, R. Smirani, G.G. Ross, *Appl. Phys. Lett.* 86 (2005) 221920.
- [19] Y.Q. Wang, R. Smirani, G.G. Ross, F. Schiettekatte, *Phys. Rev. B* 71 (2005) 161310R.